MOLECULAR AND CELLULAR BIOLOGY, Sept. 1996, p. 4798–4807 Vol. 16, No. 9
0270-7306/96/$04.00+0

Single-Stranded-DNA Binding Alters Human Replication Protein A Structure and Facilitates Interaction with DNA-Dependent Protein Kinase

LEONARD J. BLACKWELL,[1]† JAMES A. BOROWIEC,[1]* AND IRIS A. MASTRANGELO[2]*

Department of Biochemistry and Kaplan Comprehensive Cancer Center, New York University Medical Center, New York, New York 10016,[1] and Biology Department, Brookhaven National Laboratory, Upton, New York 11973[2]

Received 15 April 1996/Returned for modification 4 June 1996/Accepted 12 June 1996

Human replication protein A (hRPA) is an essential single-stranded-DNA-binding protein that stimulates the activities of multiple DNA replication and repair proteins through physical interaction. To understand DNA binding and its role in hRPA heterologous interaction, we examined the physical structure of hRPA complexes with single-stranded DNA (ssDNA) by scanning transmission electron microscopy. Recent biochemical studies have shown that hRPA combines with ssDNA in at least two binding modes: by interacting with 8 to 10 nucleotides ($hRPA_{8nt}$) and with 30 nucleotides ($hRPA_{30nt}$). We find the relatively unstable $hRPA_{8nt}$ complex to be notably compact with many contacts between hRPA molecules. In contrast, on similar lengths of ssDNA, $hRPA_{30nt}$ complexes align along the DNA and make few intermolecular contacts. Surprisingly, the elongated $hRPA_{30nt}$ complex exists in either a contracted or an extended form that depends on ssDNA length. Therefore, homologous-protein interaction and available ssDNA length both contribute to the physical changes that occur in hRPA when it binds ssDNA. We used activated DNA-dependent protein kinase as a biochemical probe to detect alterations in conformation and demonstrated that formation of the extended $hRPA_{30nt}$ complex correlates with increased phosphorylation of the hRPA 29-kDa subunit. Our results indicate that hRPA binds ssDNA in a multistep pathway, inducing new hRPA alignments and conformations that can modulate the functional interaction of other factors with hRPA.

The eukaryotic single-stranded-DNA (ssDNA)-binding protein replication protein A (RPA) plays multiple and critical roles in DNA replication, nucleotide excision repair, and homologous recombination. Two features are prominent among the currently known activities of human RPA (hRPA). hRPA stabilizes the denatured configuration of DNA and makes specific and direct contacts with multiple, functionally diverse protein partners.

Replication functions of hRPA have been extensively studied in the in vitro DNA replication system for simian virus 40, in which it is a required factor (18, 57, 58). hRPA interacts with the simian virus 40 large T antigen-origin initiation complex to stimulate origin denaturation and interacts specifically with T antigen and host DNA polymerase α-DNA primase to form a complex essential for primer synthesis (12, 42, 51, 59). During strand elongation, hRPA stimulates the action of DNA polymerases α, δ, and ε (14, 17, 27, 34, 52). Interestingly, tumor suppressor p53 may inhibit DNA replication through formation of a specific complex with hRPA, which prevents hRPA from binding to ssDNA (15). At the earliest stage of DNA nucleotide excision repair, hRPA cooperatively binds with damage recognition protein XPA and endonuclease XPG to the lesion site through direct physical interaction (11, 21, 33, 41). hRPA also greatly stimulates the activity of the human homologous pairing protein (HPP-1) and is found in a high-molecular-weight complex of recombination components (44).

hRPA exists as a stable heterotrimer of 70-, 29-, and 11-kDa subunits (18, 58). The p70 subunit is primarily responsible for binding ssDNA (28, 60). Phosphorylation of the p29 subunit in a cell-cycle-dependent manner or following DNA damage (10, 13, 37) suggests that hRPA activities are regulated through phosphorylation, although no functional effect has yet been demonstrated. Phosphorylation can be catalyzed in vitro by the cdc2-cyclin B and cdk-cyclin A complexes and by DNA-dependent protein kinase (DNA-PK) (8, 16, 19, 46). The role of the p11 subunit is less clear even though it is necessary for assembling a functional heterotrimer (22).

Heterotrimeric homologs of hRPA have been isolated from virtually every eukaryotic organism that has been tested, and characterization of the DNA-binding activities reveals significant variation (1–3, 7, 24, 43). *Saccharomyces cerevisiae* RPA binds sites of 90 to 100 nucleotides (nt) with high cooperativity (2). In contrast, two hRPA binding sites of 8 to 10 nt ($hRPA_{8nt}$) and 30 nt ($hRPA_{30nt}$) have been identified by gel shift and fluorescence quenching assays (4, 30). The $hRPA_{8nt}$ complex is detected only in the presence of glutaraldehyde, suggesting it has a weaker affinity for ssDNA than does the $hRPA_{30nt}$ complex. Overall, hRPA binds to ssDNA with a high affinity of $\sim 1 \times 10^{10}$ M^{-1}, yet binding in each complex proceeds with only moderate cooperativity (4, 29, 30). At present, the structural basis and functions of the two hRPA complexes are not known.

To better understand DNA binding and its role in heterologous interaction, we used scanning transmission electron microscopy (STEM) to examine the structures of hRPA-ssDNA complexes. Direct visualization reveals hRPA to be in elongated orientations in 30-nt complexes and closely packed in

* Corresponding author. Phone for James A. Borowiec: (212) 263-8453. Fax: (212) 263-8163. Electronic mail address: borowj01@mcrcr.med.nyu.edu. Phone for Iris A. Mastrangelo: (516) 344-3387. Fax: (516) 344-3407. Electronic mail address: mastrang@bnlux1.bnl.gov.

† Present address: Howard Hughes Medical Institute Research Laboratories, Duke University Medical Center, Durham, NC 27710.

8-nt complexes, indicating that the physical structure of each hRPA heterotrimer is likely to determine the extent of hRPA interaction with ssDNA. Furthermore, $hRPA_{30nt}$ complexes display substantial differences in configuration that depend on ssDNA length. Probing the various hRPA complexes by phosphorylation with DNA-PK reveals that hRPA undergoes significant conformational changes upon ssDNA binding. These findings indicate that hRPA binds ssDNA in multiple steps involving changes in conformation and in the potential of hRPA to interact with other factors.

MATERIALS AND METHODS

ssDNA oligonucleotides. The $d(GACT)_7GA$, $d(GACT)_{11}G$, and $d(GACT)_{20}$ oligonucleotides and the 30-bp hairpin substrate used to activate DNA-PK (5′GCACGCGGTAGCCGCCGAGGGGTCTAAAGATCTTTAGACCCCTCGGCGGCTACCGCGTGC3′) were synthesized with an Applied Biosystems 380B DNA synthesizer. Where indicated, oligonucleotides were labeled at the 5′ end with bacteriophage T4 polynucleotide kinase (U.S. Biochemicals) and [γ-^{32}P]ATP to a specific activity of 1×10^6 to 3×10^6 cpm/pmol.

hRPA and DNA-PK purification. Cultured HeLa cells were purchased from Endotronics Inc. (Minneapolis, Minn.). Cytosolic extracts were prepared and ammonium sulfate fractionation was performed as outlined previously (4). hRPA was isolated from the cytosolic extract as described by Kenny et al. (28), with the exception that Nonidet P-40 was omitted from the BN buffer in the monoQ-Sepharose chromatography step.

DNA-PK was a highly purified fraction isolated from the HeLa cell cytosolic extract. The extract was brought to 35% saturation with a saturated ammonium sulfate solution. After centrifugation, the supernatant was further precipitated by the addition of saturated ammonium sulfate solution to 65% saturation (AS65 fraction). Following overnight dialysis at 4°C against buffer A (30 mM HEPES [*N*-2-hydroxyethylpiperazine-*N*′-2-ethanesulfonic acid; pH 7.8], 0.25% [wt/vol] inositol, and 1 mM dithiothreitol [DTT]) containing 100 mM KCl, the AS65 fraction (2.1 g of protein in 23 ml) was loaded onto a 30-ml phosphocellulose column previously equilibrated with buffer A. After extensive washing with buffer A, DNA-PK was eluted with buffer A containing 0.5 M KCl. The phosphocellulose eluate (364 mg/20 ml) was dialyzed overnight (4°C) against buffer B (20 mM HEPES [pH 7.8], 1 mM EDTA, 1 mM DTT, 10% glycerol, 0.01% [vol/vol] Nonidet P-40) containing 100 mM KCl and loaded onto a 20-ml hydroxyapatite column previously equilibrated with buffer B containing 100 mM KCl. The column was washed extensively with buffer B containing 100 mM KPO_4, and DNA-PK activity was then eluted with buffer B containing 250 mM KPO_4. The hydroxyapatite eluate (108.8 mg/17 ml) was dialyzed overnight (4°C) against buffer A containing 100 mM KCl and applied to a 10-ml double-stranded-DNA–cellulose column (U.S. Biochemicals). After washing the column sequentially with buffer A containing 50 mM KCl and buffer A containing 100 mM KCl, DNA-PK activity was eluted with buffer A containing 500 mM KCl (26.8 mg/4 ml). The specific activity of the final DNA-PK fraction was 3 U/mg (35). The appearance of the 70- and 86-kDa phosphoproteins in our kinase assays indicated that the DNA-PK fraction contained the Ku autoantigen.

DNA-PK activity was assayed during purification by measuring the phosphorylation of the hRPA p29 subunit. Briefly, reaction mixtures (30 μl) containing 300 ng of hRPA, 50 ng of M13 ssDNA, 30 mM HEPES (pH 7.8), 10 mM $MgCl_2$, 1 mM DTT, 50 μM [γ-^{32}P]ATP (at $\sim 5 \times 10^7$ cpm/μmol), and aliquots of the column fraction to be assayed were incubated at 37°C for 10 min. The reactions were quenched by the addition of 20 μl of sodium dodecyl sulfate-polyacrylamide gel electrophoresis (SDS-PAGE) loading buffer (50 mM Tris-HCl [pH 6.8], 100 mM DTT, 2% SDS, 0.1% bromophenol blue, and 10% glycerol). Reaction products were separated by SDS-PAGE through a 15% polyacrylamide gel (acrylamide-bisacrylamide, 80:1) and visualized by autoradiography. When necessary, phosphorylated hRPA was identified by Western blotting (immunoblotting) with an anti-p29 antibody (28).

Binding reactions used for STEM analysis. Binding reactions were essentially as described previously (4), except bovine serum albumin was omitted from the binding buffer. Briefly, reaction mixtures (20 μl) contained 30 mM HEPES (pH 7.8), 7 mM $MgCl_2$, 0.5 mM DTT, 0.5 pmol of the ssDNA substrate of the desired length, and 2.8 pmol of hRPA. ϕX174-hRPA reaction mixtures contained 300 ng of hRPA and 10 ng of the ϕX174 plus strand (Gibco-BRL). At lower hRPA concentrations, bare regions of DNA were visible. Reaction mixtures were incubated at 37°C for 10 min. For examination of the $hRPA_{8nt}$ complex, reaction mixtures were subsequently adjusted to 0.1% glutaraldehyde and incubated an additional 10 min at 37°C. A 5-μl aliquot was immediately removed and prepared for STEM analysis.

Aliquots of each reaction mixture were adsorbed for 1 min on carbon-coated titanium grids that had been discharged in air and coated with poly-L-lysine as described previously (40). STEM grids were then washed with 20 mM ammonium acetate and immersed in liquid nitrogen, followed by overnight sublimation. EM preparations of ϕX174-hRPA were stained with uranyl acetate and rotary shadowed with tungsten after the wash step (39). For cross-linking of hRPA complexes on the STEM grid, 5-μl aliquots of reaction mixtures were adsorbed for 1 min and removed, and then 5 μl of 0.1% glutaraldehyde was added for 2 min. Grids were washed and treated subsequently as described above.

The principles of STEM mass measurement and data analysis have been described previously (40, 54). Briefly, a 2.5-Å (0.25-nm)-diameter electron beam scans protein complexes on a thin carbon foil in a 10-Å (1-nm) raster pattern. The number of electrons scattered is proportional to the mass of the constituent atoms. Calibration procedures compensate for any loss of mass due to electron beam damage.

Phosphorylation of hRPA by DNA-PK. Reaction mixtures (30 μl) containing 30 mM HEPES (pH 7.8), 10 mM $MgCl_2$, 1 mM DTT, 50 μM [γ-^{32}P]ATP (at $\sim 5 \times 10^7$ cpm/μmol), 1 ng of hairpin substrate, 1 to 50 ng of ssDNA substrate (using oligonucleotides of the desired length or M13 ssDNA), 300 ng of hRPA or α-casein, and 20 μg of the DNA-PK-containing fraction were incubated at 37°C for 10 min. The reactions were stopped by the addition of SDS-PAGE loading buffer. Phosphorylated proteins were separated by SDS-PAGE through a 15% polyacrylamide gel (acrylamide-bisacrylamide, 80:1) and visualized by autoradiography. Bands corresponding to α-casein or the p29 subunit of hRPA were excised from the gel, and the radioactivity present was measured by scintillation counting.

Reactions monitoring the complexes of phosphorylated hRPA with ssDNA were similar to those described above. From each reaction mixture, 15 μl was used for analysis by SDS-PAGE as described above. The remaining 15 μl was analyzed by electrophoresis through a native 8% polyacrylamide gel (acrylamide-bisacrylamide, 80:1). Native gels were electrophoresed at 12 V/cm in 89 mM Tris–89 mM boric acid–2 mM EDTA buffer. The phosphorylated hRPA p29 subunit was visualized by autoradiography.

Phosphorylation of hRPA in the presence of ^{32}P-labeled ssDNA substrates was performed as described above except [γ-^{32}P]ATP was not included in the reaction mixture. Equal counts of either a 45-nt or an 80-nt substrate (~0.5 ng of ssDNA substrate) were incubated with increasing amounts of cold oligonucleotide (i.e., 1, 5, 10, 25, or 50 ng). hRPA-ssDNA complexes were separated by native gel electrophoresis as described above and examined by autoradiography.

RESULTS

Formation of elongated or globular oligomers on ssDNAs. The relationship between the $hRPA_{8nt}$ and $hRPA_{30nt}$ complexes was examined by using STEM to provide detailed molecular images and accurate molecular masses (39, 40). Viewing hRPA complexes within 0.512-μm fields showed that incubation of hRPA with a 45-nt (Fig. 1B) or an 80-nt (Fig. 1C) substrate in the absence of glutaraldehyde caused hRPA to localize into structures that were elongated compared with the uncomplexed state (Fig. 1A). Glutaraldehyde-treated complexes, however, were not elongated but rather were distinctly globular and increased in diameter as the ssDNA length increased (Fig. 1E and F).

STEM mass measurements show that with each length of ssDNA examined, a higher degree of oligomerization distinguished cross-linked from non-cross-linked complexes (Fig. 2). Detection of hRPA oligomers was dependent on the presence of ssDNA, either with or without glutaraldehyde (Fig. 2A and E). Thus, hRPA does not aggregate or oligomerize nonspecifically to any significant degree under our experimental conditions. In the absence of cross-linking, on 30-, 45-, and 80-nt substrates the prominent hRPA complexes corresponded to a monomer, a dimer, and a trimer of the hRPA heterotrimer, respectively (Fig. 2B to D). The presence of a 227-kDa peak on the 45-nt substrate, corresponding to an hRPA dimer with a predicted molecular mass of 235 kDa, indicates that under conditions favoring the formation of the $hRPA_{30nt}$ complex, hRPA is capable of binding ssDNA by a binding site of approximately 22 nt.

Subsequent to glutaraldehyde cross-linking, up to five hRPA molecules were found associated with the 45-nt substrate and up to seven hRPA molecules were associated with the 80-nt substrate, although the average oligomer size was smaller (Fig. 2F to H). It is unlikely that tight packing and oligomerization of hRPA are merely due to glutaraldehyde-cross-linked aggregates which associate secondarily with an $hRPA_{30nt}$ complex. Previous studies employing glutaraldehyde indicated that the

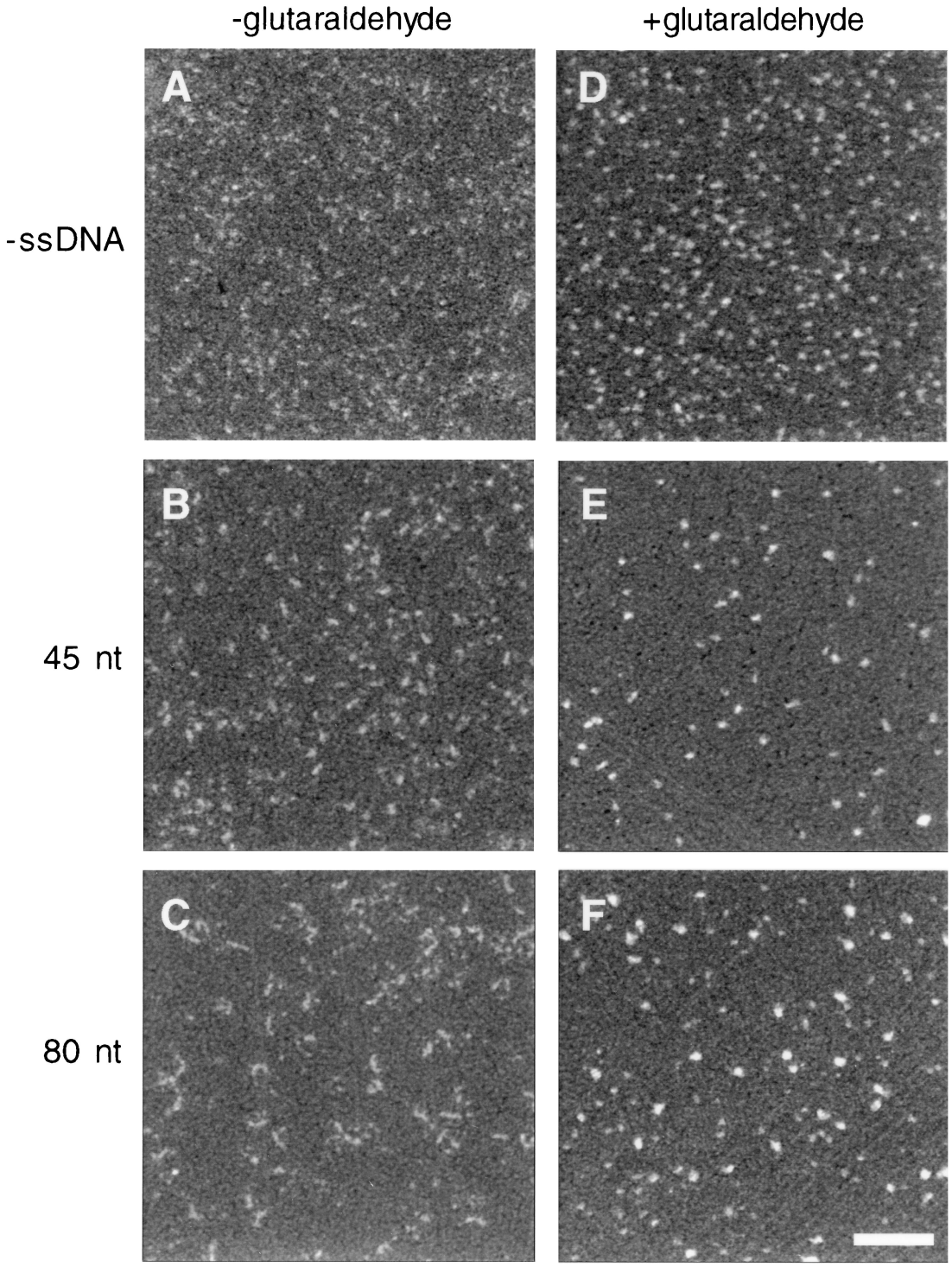

FIG. 1. STEM detects elongated or globular hRPA-ssDNA complexes. hRPA was incubated alone (A and D) or in the presence of 45-nt (B and E) or 80-nt (C and F) ssDNA. STEM images of complexes subjected to glutaraldehyde cross-linking (D to F) and of untreated complexes (A to C) are shown. Fields are 0.512 μm. Bar, 100 nm.

binding of additional hRPA heterotrimers is tightly coupled to 8-nt increases in DNA length over a 50-nt range (4). Thus, molecular mass and image data provided by STEM demonstrate that distinct stoichiometries and configurations distinguish the $hRPA_{30nt}$ complexes from the $hRPA_{8nt}$ complexes.

Coexistence of $hRPA_{8nt}$ and $hRPA_{30nt}$ complexes in solution. A plausible explanation for the formation of two distinct structural complexes is that the $hRPA_{8nt}$ complex is a precursor of the $hRPA_{30nt}$ complex. During preparation of the STEM grids, the more unstable $hRPA_{8nt}$ complex is lost. If this hy-

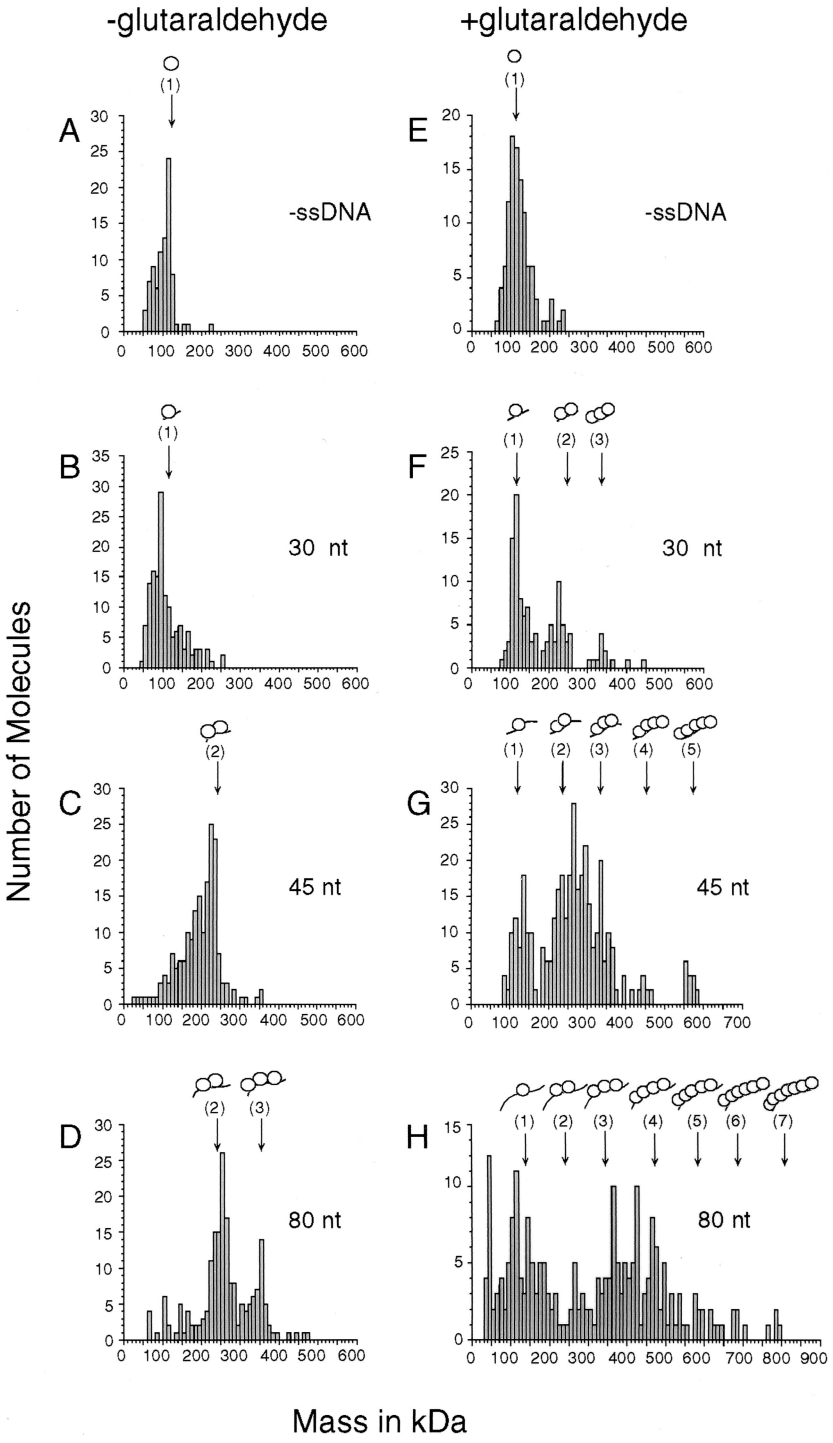

FIG. 2. Different oligomeric states of $hRPA_{30nt}$ and $hRPA_{8nt}$ complexes are identified by STEM mass measurement. hRPA was incubated alone (A and E) or with 30-nt (B and F), 45-nt (C and G), or 80-nt (D and H) substrate. $hRPA_{8nt}$ or $hRPA_{30nt}$ complexes were prepared in the presence (E to H) or absence (A to D), respectively, of glutaraldehyde cross-linking. In each experiment, the molecular masses of approximately 100 to 200 randomly chosen molecules were measured. Arrows above each histogram indicate the expected masses of oligomeric complexes including ssDNA. Stoichiometry is also indicated in schematic form.

pothesis is correct, then the two complexes should coexist in solution. Taking advantage of the method of preparing hRPA molecules for STEM analysis, we tested this possibility. Binding reaction mixtures were prepared in the absence of glutaraldehyde and applied to a STEM grid where hRPA and the hRPA-ssDNA complexes that have assembled adhere to carbon. Glutaraldehyde was then added to cross-link the existing hRPA-ssDNA complexes. With the exception of adding glutaraldehyde to the grid, the protocol is identical to that used to identify $hRPA_{30nt}$ complexes.

Cross-linking on the STEM grid revealed the presence of significant numbers of hRPA dimers and trimers (Fig. 3), oligo-

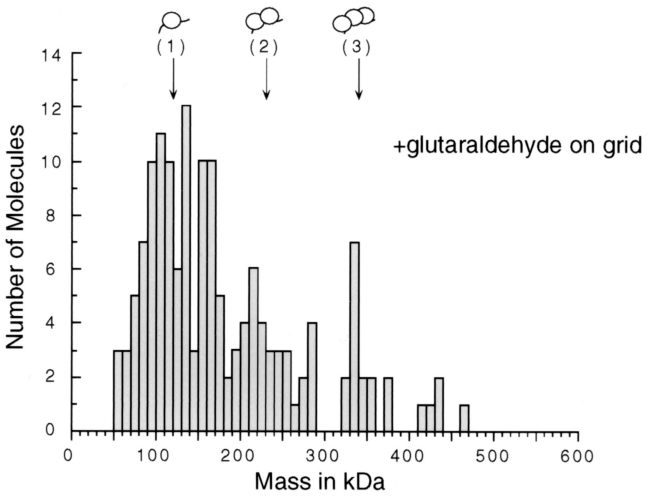

FIG. 3. The $hRPA_{8nt}$ and $hRPA_{30nt}$ complexes coexist in solution. hRPA was incubated with 30-nt ssDNA in the absence of glutaraldehyde. Complexes were subjected to glutaraldehyde cross-linking on the grid as described in Materials and Methods. The histogram shows that molecular masses of hRPA-ssDNA oligomers observed under these conditions include $hRPA_{8nt}$ complexes. Arrows and drawings indicate the stoichiometry of possible oligomeric complexes.

meric states that are consistent with the presence of $hRPA_{8nt}$ complexes. Use of 45- or 80-nt substrates in this procedure similarly indicated the simultaneous presence of the $hRPA_{8nt}$ and $hRPA_{30nt}$ complexes (data not shown). We therefore conclude that the $hRPA_{8nt}$ and $hRPA_{30nt}$ complexes are simultaneously present in solution, a finding consistent with the hypothesis that the $hRPA_{8nt}$ complex is a precursor of the $hRPA_{30nt}$ complex.

$hRPA_{30nt}$ complexes exist as extended and contracted structures. Images of $hRPA_{30nt}$ complexes revealed distinct physical differences in component hRPA molecules that depended on the length of the ssDNA substrate (Fig. 4A). Relatively extended dimers were formed on the 80-nt substrate, while more-contracted dimers were formed on the 45-nt substrate. Contacts between monomers in contracted dimers are more apparent than those between monomers in extended dimers. The overall elongated configurations of dimer and trimer complexes observed on the 80-nt substrate suggest that hRPA molecules are aligned along the DNA backbone.

We measured the lengths of numerous complexes and verified the contracted nature of the $hRPA_{30nt}$ dimers (Fig. 4B). hRPA monomers, in the absence of ssDNA, were roughly globular and had an average length ($\pm$ standard deviation) of 11.7 $\pm$ 2.5 nm. This value is in close agreement with the previously determined Stokes radius of ~5.3 nm (29, 58). hRPA dimer length on the 45-nt substrate measured 19.2 $\pm$ 2.7 nm and was significantly shorter than the average dimer length of 30.1 $\pm$ 2.9 nm on the 80-nt substrate. For comparison, the average length of hRPA trimers, 35.0 $\pm$ 3.3 nm on the latter substrate, was only slightly longer and equaled the length of three monomers. We conclude that alterations in the DNA length can cause hRPA to undergo either a reorientation with respect to the DNA axis or a significant conformational change, although these possibilities are nonexclusive.

In the presence of glutaraldehyde cross-linking, we observed densely packed heterotrimer structures regardless of the oligomeric state (Fig. 4C). In these $hRPA_{8nt}$ complexes, DNA contacts are presumably reduced compared with the elongated $hRPA_{30nt}$ complexes. Thus, contacts between tightly packed hRPA molecules may facilitate association of hRPA with the DNA. STEM images also indicate that homologous hRPA contacts and the ssDNA substrate length influence the conformational alignment of hRPA in the DNA-binding complex.

hRPA conformational changes induced upon binding ssDNA. In order to test for possible conformational changes, we biochemically probed hRPA oligomers bound to ssDNA with DNA-PK, which is known to phosphorylate the hRPA p29 subunit (8, 46). We devised a novel assay in which changes in hRPA phosphorylation specifically induced upon ssDNA binding could be monitored, thereby indicating an altered conformation.

The experiment is based on the activation of DNA-PK independent of the ssDNA used for hRPA binding. Although DNA-PK activation requires DNA binding, protein substrates can be phosphorylated either in *cis* or in *trans* (20, 26, 45). We used a 30-bp hairpin substrate, a DNA molecule for which hRPA has little affinity, to potently activate DNA-PK. The activated DNA-PK will then act in *trans* on free hRPA, hRPA-ssDNA complexes, or an α-casein control (Fig. 5A).

We found that hRPA became phosphorylated by the activated DNA-PK in a reaction dependent upon ssDNA (Fig. 5B). hRPA phosphorylation was stimulated three- to fourfold by the 45-nt substrate compared with reaction mixtures lacking ssDNA or containing substrates 24 or 30 nt in length. The use of ssDNA substrates longer than 45 nt did not further increase hRPA phosphorylation. Importantly, the phosphorylation of α-casein, which does not bind DNA, was unaffected by any ssDNA length. The specific ssDNA-dependent increase in hRPA phosphorylation therefore demonstrates that hRPA undergoes a conformational transition upon binding ssDNA.

Differential phosphorylation of hRPA oligomers on ssDNA by DNA-PK. We subsequently tested whether the hRPA oligomeric state influences the extent of phosphorylation by examining the phosphorylation of hRPA oligomers bound to 45- and 80-nt substrates (Fig. 6). For each length tested, we titrated ssDNA against a constant level of hRPA to produce several oligomeric complexes. Experiments were performed independently in the presence of either [γ-^{32}P]ATP or [^{32}P] ssDNA to monitor the protein or the DNA, respectively, in each hRPA oligomer. Partitioning of phosphorylated hRPA into distinct oligomers was observed by native gel electrophoresis (Fig. 6B and C), and total p29 phosphorylation was detected by denaturing gel electrophoresis (Fig. 6A).

Interestingly, hRPA phosphorylation displayed distinct differences relative to the oligomeric state (Fig. 6A and B). For both substrates, hRPA phosphorylation was inversely proportional to the number of protein molecules bound to the ssDNA. In reaction mixtures containing 50 ng of the 45-nt substrate, the hRPA/45 nt molar ratio is ~1:1 and hRPA bound primarily as a monomer (Fig. 6B and C). The monomeric complex correlates with the greatest stimulation in hRPA phosphorylation on the 45-nt substrate (Fig. 6A). In 10-ng reaction mixtures, the hRPA/45 nt molar ratio increases to ~5:1, similar to that used with STEM, and resulted in the binding of hRPA dimers (Fig. 6B and C). Notably, phosphorylation of dimers on the 45-nt substrate decreased between 5- and 10-fold compared with monomers. In contrast, similar stoichiometric changes with the 80-nt substrate resulted in a less than twofold difference in phosphorylation.

It is clear that formation of dimeric complexes on the 45-nt substrate correlates with a substrate-specific reduction in hRPA phosphorylation. Therefore, these data, together with the STEM image data, indicate that hRPA phosphorylation sites are relatively inaccessible on contracted dimers while extended oligomers expose these sites to phosphorylation by DNA-PK. The structural alterations we observe may influence

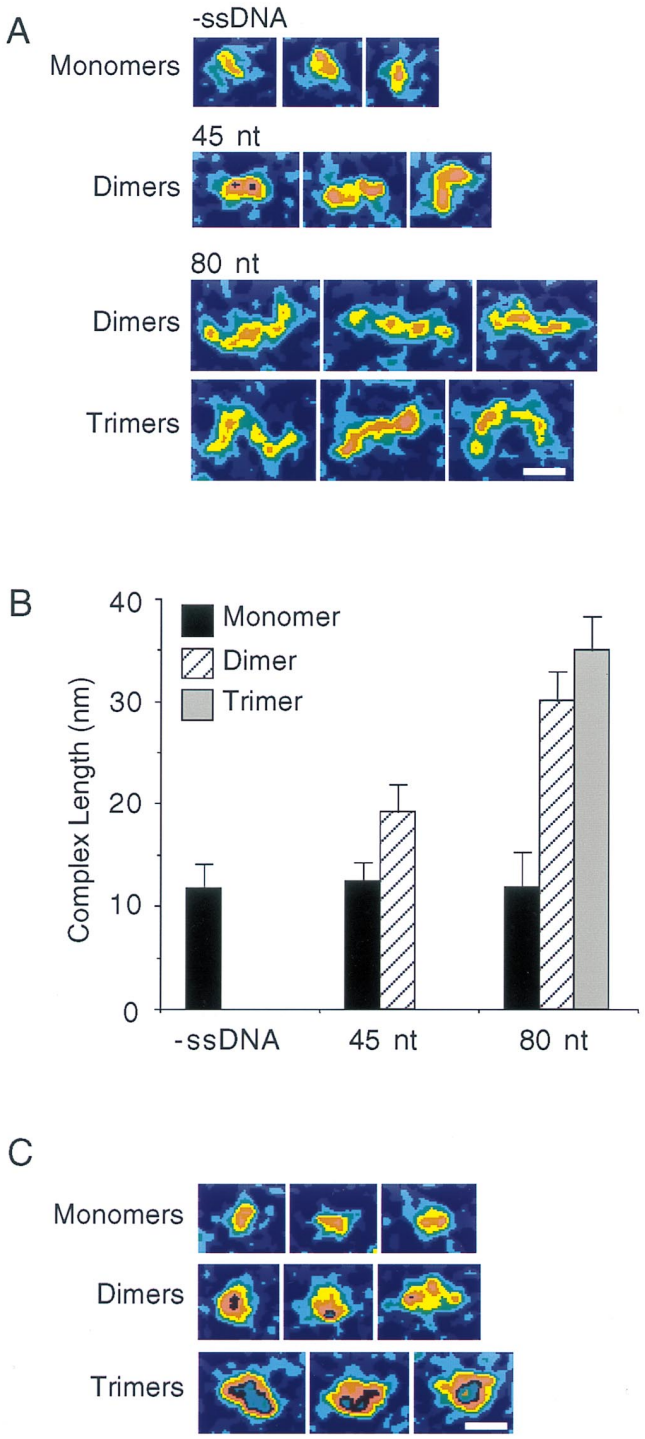

FIG. 4. Distinct configurations in $hRPA_{30nt}$ and $hRPA_{8nt}$ oligomers are visualized by STEM. Oligomers of the $hRPA_{30nt}$ and $hRPA_{8nt}$ complexes are shown in close-up views. Images of representative molecules are built from scattered electron counts that have been interpolated, averaged, and color coded. The colors change progressively through cyan, green, yellow, orange, pink, and black cycles. Each color change represents a five-count increase above carbon background and equals 500 Da/1.00 nm^2. Stoichiometries, noted to the left of each panel, were determined from the mass histograms in Fig. 2. (A) Elongated $hRPA_{30nt}$ complexes form in the absence of glutaraldehyde. Oligomers on 45- and 80-nt substrates are shown, as are hRPA molecules not bound to ssDNA. (B) Length measurements of hRPA and $hRPA_{30nt}$ complexes. The bar graph shows the average lengths and standard deviations (error bars) of approximately 100 to 200 molecules, identified by stoichiometry and taken from reactions in panel A. The analysis indicates the presence of contracted $hRPA_{30nt}$ dimers on 45-nt substrate and extended $hRPA_{30nt}$ dimers on 80-nt substrate. (C) Compact, globular $hRPA_{8nt}$ dimers and other oligomers are detected on 80-nt substrate in the presence of glutaraldehyde. Bars, 10 nm (A and C).

the accessibility of phosphorylation sites by promoting subtle conformational changes as well as unblocking the sites through mass realignments.

Formation of $hRPA_{30nt}$ complexes on long ssDNA. In order to assess the generality of the hRPA molecular interactions observed on short oligonucleotides, we also examined complexes formed on the 5,386-nt circular ϕX174 ssDNA. Reaction mixtures contained an hRPA/nucleotide molar ratio of ~1:10, and glutaraldehyde cross-linking was omitted. Among hRPA-ϕX174 complexes, a fraction appeared as quasiplanar circles whose mean contour lengths measured 1,600 ± 205 nm (Fig. 7A and B). This corresponds to 90% of the length of double-stranded ϕX174 and differs from the fourfold compaction of DNA that *S. cerevisiae* RPA complexes produce upon similar analysis (2). The average mass of hRPA-ϕX174 complexes determined by STEM was 18.1 ± 2.8 MDa (Fig. 7C and D). Dividing the total mass by the total length yields a mass of 113 kDa per 10 nm around the hRPA-ϕX174 complex. In selected regions of the complex, we measured mass as a function of length and determined a similar value of 101 kDa per 10 nm (Fig. 7E and F). The mass per unit length in hRPA-ϕX174 complexes is in agreement with the value of 116 kDa per 11 nm found for $hRPA_{30nt}$ monomer and trimer complexes on oligonucleotides, shown in Fig. 4B.

These results indicate that in the absence of cross-linking, hRPA does not form higher-order structures when associating with long ssDNA. Therefore, the $hRPA_{30nt}$ complex appears to be the stable modular unit in binding both very long and very short regions of ssDNA.

DISCUSSION

We have examined the binding of hRPA to ssDNA both visually, by STEM, and biochemically, by using DNA-PK as a probe of hRPA conformation. Physical evidence in STEM images directly shows that hRPA heterotrimers interact with ssDNA in at least three distinct configurations. Elongated complexes replace compact complexes as the DNA contact size increases from ~8 to ~30 nt, marking a concurrent, functional transition to stable DNA binding. Binding data for oligonucleotides and long DNA indicate that the increased site size in the $hRPA_{30nt}$ complex is not a consequence of DNA wrapping around the protein, as is found for *Escherichia coli* ssDNA-binding protein (SSB) (38). Rather, the hRPA heterotrimer itself reorients and elongates on ssDNA, thereby altering the extent of contact with the ssDNA. Elongated molecules exist in either a contracted or an extended form, depending on ssDNA length and the degree of hRPA oligomerization. Formation of oligomers with extended orientation coordinates precisely with more efficient phosphorylation by DNA-PK. Taken together, these data indicate that hRPA binds ssDNA by first utilizing a small binding site on DNA which is subsequently enlarged to produce a stable hRPA-ssDNA complex. The biochemical and structural data support the conclusion that hRPA undergoes a significant conformational change during the pathway to stable ssDNA binding.

The induction of hRPA conformational changes upon ssDNA binding is deduced from the sensitivity of hRPA to phosphorylation by DNA-PK. Although others have shown that DNA-PK phosphorylates hRPA, no direct effect of ssDNA binding on the intrinsic hRPA reactivity to DNA-PK was noted (8, 46).

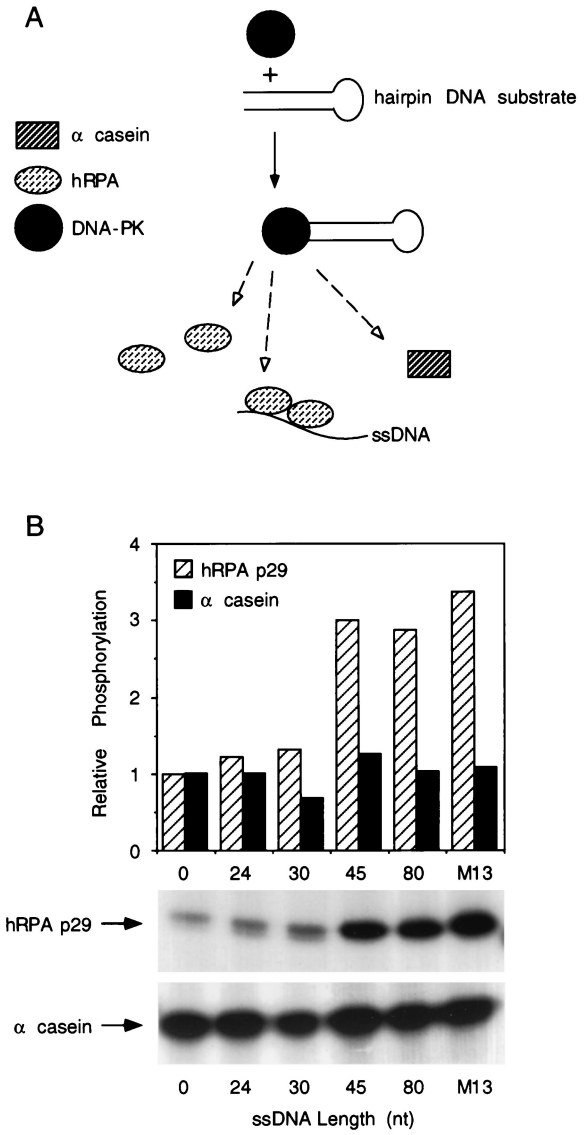

FIG. 5. Specific stimulation of hRPA phosphorylation by activated DNA-PK depends on ssDNA length. (A) Diagram depicts the *cis* activation of DNA-PK by a 30-bp hairpin DNA and the *trans* phosphorylation of free hRPA, hRPA bound to ssDNA, or α-casein by the activated DNA-PK. (B) Phosphorylation of the hRPA p29 subunit or α-casein in the presence of ssDNA substrates of increasing length. As described in Materials and Methods, reaction mixtures contained 300 ng of hRPA or α-casein, 1 ng of the hairpin DNA, 50 ng of ssDNA substrate (24, 30, 45, or 80 nt in length, or M13 ssDNA), and DNA-PK. Reaction products were separated by denaturing gel electrophoresis and visualized by autoradiography. The hRPA p29 subunit is visible as two differentially phosphorylated bands. Phosphorylated bands corresponding to the hRPA p29 subunit or α-casein were excised from the gel, and the radioactivity was measured by scintillation counting. The bar graph represents the fold change above the background observed for each kinase substrate in the absence of ssDNA.

In these cases, ssDNA templates were used that could both stimulate DNA-PK activity and allow hRPA binding, thus masking detection of hRPA conformational changes. Separation of these activities was made possible in our assays by the use of two structurally distinct DNA molecules: a 30-bp hairpin DNA that potently activates DNA-PK but does not bind hRPA, and the ssDNA substrate for hRPA binding that is not an effective stimulator of DNA-PK activity.

Significant increases in hRPA phosphorylation were observed when hRPA was incubated with ssDNA consisting of more than 30 nt. The increased affinity of hRPA for longer DNA molecules can only partly explain this length dependence. Rather, we demonstrate that differences in phosphorylation among oligomers directly correlate with STEM observations that hRPA binds ssDNA in distinct configurations depending on oligonucleotide length. Using conditions that favor detection of the $hRPA_{30nt}$ complex, the length of monomers in dimer complexes on the 45-nt substrate was ~35% shorter than on the 80-nt substrate and ~20% shorter than hRPA monomers without ssDNA. Furthermore, hRPA dimer complexes bound to the 45-nt substrate were relatively underphosphorylated compared with monomers on the 45-nt substrate. The contracted configuration of hRPA dimers observed by STEM suggests that hRPA phosphorylation sites are relatively inaccessible to DNA-PK. Therefore, our biochemical and structural data indicate that specific conformational changes are induced in hRPA upon binding to ssDNA in an extended $hRPA_{30nt}$ complex.

Our studies utilize DNA-PK as a probe of hRPA conformation and do not directly bear on the role of hRPA phosphorylation by DNA-PK. hRPA is essential for both excision nucleotide repair and simian virus 40 DNA replication, but in vitro reconstitution studies have not shown any significant effects of hRPA phosphorylation on these processes (8, 23, 32, 47). However, it is clear that the major effect of cellular DNA-PK loss is to render a cell defective in double-strand DNA break repair and V(D)J recombination (5, 31, 36, 48–50). DNA-PK-deficient cells are defective in radiation-induced phosphorylation of hRPA, but the functional consequences are unknown at present (6). Thus, determining the biological effects of hRPA phosphorylation by DNA-PK requires additional information concerning the role of hRPA in the latter processes.

Wold and colleagues have suggested that in the $hRPA_{30nt}$

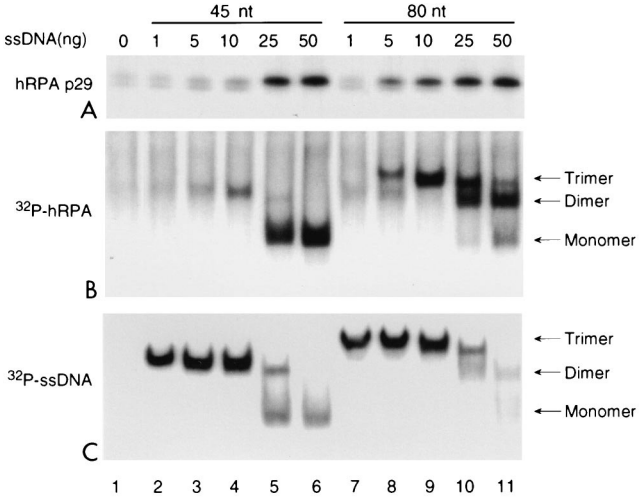

FIG. 6. Stimulation of hRPA phosphorylation on 45-nt substrate varies with the oligomeric state of the $hRPA_{30nt}$ complex. Phosphorylation reactions using DNA-PK were carried out as described in the legend to Fig. 5 but with increasing amounts of 45- or 80-nt substrate. Total p29 phosphorylation (A) was visualized by denaturing gel electrophoresis and autoradiography. Phosphorylated bands were excised from the gel, and the radioactivity was measured by scintillation counting. Values for phosphate incorporated, above the background level found in the absence of ssDNA, were 0.30 pmol (lane 3), 0.58 pmol (lane 4), 2.9 pmol (lane 6), 1.9 pmol (lane 8), 2.5 pmol (lane 9), and 3.7 pmol (lane 11). Native complexes containing either [^{32}P]hRPA (B) or [^{32}P]ssDNA (C) were detected by nondenaturing gel electrophoresis and autoradiography.

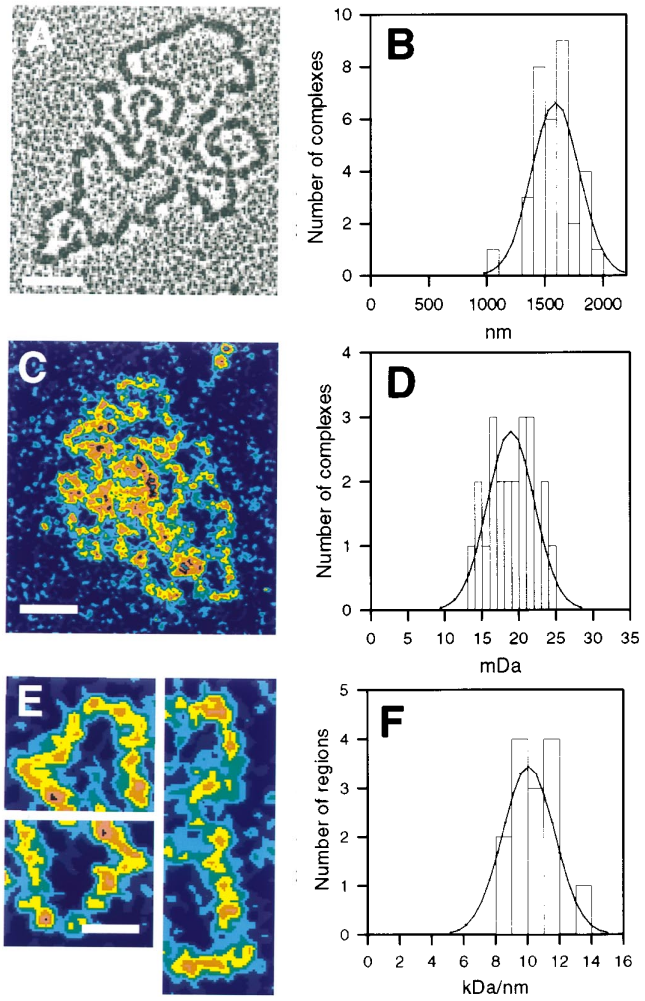

FIG. 7. Contour length, molecular mass, and mass per unit length of hRPA-ϕX174 complexes. Means ± standard deviations are given for Gaussian distributions fitted to histograms. (A and B) Contour lengths were measured from conventional EM images of planar complexes, such as that shown, and equal 1,600 ± 205 nm (n = 34). (C and D) Molecular masses of complexes similar to that depicted were determined by STEM to be 18.1 ± 2.8 MDa (n = 22). The hRPA component of the complex is therefore equivalent to ~160 hRPA heterotrimers. Using the mean values in panels B and D, we obtain 11.3 kDa/nm as the predicted mass per unit length. (E and F) Mass per unit length was directly measured from sections of hRPA-ϕX174 complexes that were free of overlaps, such as the sections shown. The measured value is 10.1 ± 1.6 kDa/nm (n = 14). Bars, 60 nm (A), 40 nm (C), and 13 nm (E).

binding mode, hRPA requires at least 20 nt of ssDNA contacted per monomer and approximately 10 nt between monomers for stable complex formation (29). We observe that binding of hRPA to ssDNA substrates that prevent complete monomeric occlusion of 30 nt constrains hRPA to bind the DNA in an altered form. The hRPA bound to these size-restricted ssDNA molecules is observably compact and shorter. STEM images additionally suggest that the contracted hRPA dimers have increased contact between hRPA monomers. The altered structures most likely account for the unusual gel shift properties of hRPA bound to relatively short ssDNA molecules (<45 nt), which previously led to the prediction that such complexes are relatively compact (4). Thus, hRPA does not simply bind ssDNA in 30-nt steps but can bind in distinct orientations depending on the available length of ssDNA.

By carrying out glutaraldehyde cross-linking on the STEM grid (Fig. 3), we trapped $hRPA_{8nt}$ and $hRPA_{30nt}$ complexes together, indicating that both exist in solution. In the absence of cross-linking, the less stable $hRPA_{8nt}$ complex is lost under the conditions used to prepare the STEM grids as well as those under which electrophoretic gels were run (4). The simplest explanation for the coexistence of these two complexes is that the $hRPA_{8nt}$ complex is a precursor of the $hRPA_{30nt}$ complex. In this view, the $hRPA_{8nt}$ and the $hRPA_{30nt}$ complexes are the extremes of a continuum defining the pathway of hRPA-ssDNA complex formation.

Model of hRPA binding to ssDNA. Our data led to a model for a multistep pathway for binding of hRPA to ssDNA (Fig. 8). Rather than contacting 20 to 30 nt of ssDNA in a single step, hRPA first contacts the ssDNA unstably, utilizing an 8- to 10-nt binding site in a compact $hRPA_{8nt}$ complex. As this complex appears to bind ssDNA with moderate cooperativity (4), increased stability is achieved by the binding of an additional hRPA monomer (Fig. 8A). In the presence of a sufficient length of ssDNA, hRPA undergoes a topological reorientation and makes additional contacts along the ssDNA (Fig. 8B). This intermediate hRPA-ssDNA complex is relatively contracted and exhibits significant interaction between hRPA monomers as revealed by STEM. In the final stage of hRPA binding, hRPA fully extends along the ssDNA to form a stable $hRPA_{30nt}$ complex (Fig. 8C). During this last stage, hRPA undergoes a significant conformational change that can result in both productive interaction with DNA-PK and, likely, additional DNA metabolic factors (Fig. 8D). The prominent hRPA-hRPA interactions we observe in unstable $hRPA_{8nt}$ complexes create a localized pool of protein available for quick mobilization into more stable binding forms or for interaction with other replication and repair factors.

Conformational changes have been implicated in the function of a number of viral and bacterial SSBs. Contiguous binding of bacteriophage T4 gene 32 protein and *E. coli* SSB elicits

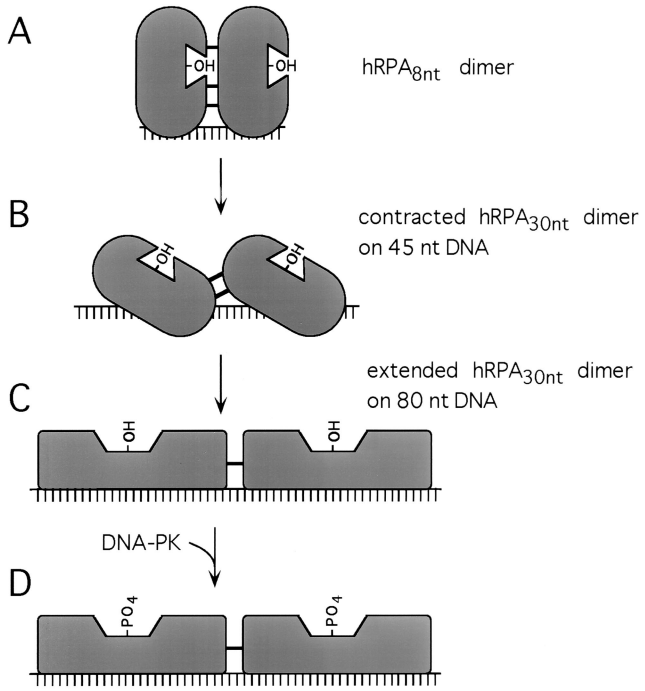

FIG. 8. Model of hRPA binding to ssDNA. See the text for a description of the model.

exposure of a specific protein domain (25, 55, 56). A proteolytic product of gene 32 protein lacking this region, although unaffected in ssDNA binding, is functionally impaired in T4 DNA replication and is unable to interact with several T4-encoded proteins (9). The X-ray crystal structure of the DNA-binding domain of the adenovirus DNA-binding protein shows a highly conserved region that is flexible and may fold when DNA is contacted (53). hRPA is perhaps unique in undergoing DNA-dependent structural transitions that are accompanied by observable alterations in appearance. That hRPA undergoes structural changes upon ssDNA binding which modulate homologous- and heterologous-protein interactions suggests that this attribute is universal among SSBs.

ACKNOWLEDGMENTS

We thank members of the Borowiec laboratory for constructive comments during the course of this project; Joe Wall, director of the Brookhaven STEM, for his unfailing support; Paul Hough for his generous help and advice; and Brett Bloom for assistance in the latter part of the investigation.

This research was supported by NIH grant AI29963 and a Kaplan Cancer Center Developmental Funding and Kaplan Cancer Center Support Core Grant (NCI P30CA16087) (J.A.B.) and by the Department of Energy Office of Health and Environmental Research (I.A.M.). The Brookhaven STEM is an NIH Biotechnology Resource (RR0177).

REFERENCES

1. **Adachi, Y., and U. K. Laemmli.** 1992. Identification of nuclear pre-replication centers poised for DNA synthesis in Xenopus egg extracts: immunolocalization study of replication protein A. J. Cell Biol. **119:**1–15.
2. **Alani, E., R. Thresher, J. Griffith, and R. D. Kolodner.** 1992. Characterization of DNA-binding and strand-exchange stimulation properties of y-RPA, a yeast single-strand-DNA-binding protein. J. Mol. Biol. **227:**54–71.
3. **Atrazhev, A., S. Zhang, and F. Grosse.** 1992. Single-stranded DNA binding protein from calf thymus. Purification, properties, and stimulation of the homologous DNA-polymerase-alpha-primase complex. Eur. J. Biochem. **210:**855–865.
4. **Blackwell, L. J., and J. A. Borowiec.** 1994. Human replication protein A binds single-stranded DNA in two distinct complexes. Mol. Cell. Biol. **14:** 3993–4001.
5. **Blunt, T., N. J. Finnie, G. E. Taccioli, G. C. M. Smith, J. Demengeot, T. M. Gottlieb, R. Mizuta, A. J. Varghese, F. W. Alt, P. A. Jeggo, and S. P. Jackson.** 1995. Defective DNA-dependent protein kinase activity is linked to V(D)J recombination and DNA repair defects associated with the murine *scid* mutation. Cell **80:**813–823.
6. **Boubnov, N. V., and D. T. Weaver.** 1995. *scid* cells are deficient in Ku and replication protein A phosphorylation by the DNA-dependent protein kinase. Mol. Cell. Biol. **15:**5700–5706.
7. **Brill, S. J., and B. Stillman.** 1989. Yeast replication factor-A functions in the unwinding of the SV40 origin of replication. Nature (London) **342:**92–95.
8. **Brush, G. S., C. W. Anderson, and T. J. Kelly.** 1994. The DNA-activated protein kinase is required for the phosphorylation of replication protein A during simian virus 40 DNA replication. Proc. Natl. Acad. Sci. USA **91:** 12520–12524.
9. **Burke, R. L., B. M. Alberts, and J. Hosoda.** 1980. Proteolytic removal of the COOH terminus of the T4 gene 32 helix-destabilizing protein alters the T4 in vitro replication complex. J. Biol. Chem. **255:**11484–11493.
10. **Carty, M. P., M. Zernik-Kobak, S. McGrath, and K. Dixon.** 1994. UV light-induced DNA synthesis arrest in HeLa cells is associated with changes in phosphorylation of human single-stranded DNA-binding protein. EMBO J. **13:**2114–2123.
11. **Coverley, D., M. K. Kenny, M. Munn, W. D. Rupp, D. P. Lane, and R. D. Wood.** 1991. Requirement for the replication protein SSB in human DNA excision repair. Nature (London) **349:**538–541.
12. **Dean, F. B., P. Bullock, Y. Murakami, C. R. Wobbe, L. Weissbach, and J. Hurwitz.** 1987. Simian virus 40 (SV40) DNA replication: SV40 large T antigen unwinds DNA containing the SV40 origin of replication. Proc. Natl. Acad. Sci. USA **84:**16–20.
13. **Din, S., S. J. Brill, M. P. Fairman, and B. Stillman.** 1990. Cell-cycle-regulated phosphorylation of DNA replication factor A from human and yeast cells. Genes Dev. **4:**968–977.
14. **Dornreiter, I., L. F. Erdile, I. U. Gilbert, D. von Winkler, T. J. Kelly, and E. Fanning.** 1992. Interaction of DNA polymerase α-primase with cellular replication protein A and SV40 T antigen. EMBO J. **11:**769–776.
15. **Dutta, A., J. M. Ruppert, J. C. Aster, and E. Winchester.** 1993. Inhibition of DNA replication factor RPA by p53. Nature (London) **365:**79–82.
16. **Dutta, A., and B. Stillman.** 1992. cdc2 family kinases phosphorylate a human cell DNA replication factor, RPA, and activate DNA replication. EMBO J. **11:**2189–2199.
17. **Erdile, L. F., W. D. Heyer, R. Kolodner, and T. J. Kelly.** 1991. Characterization of a cDNA encoding the 70-kDa single-stranded DNA-binding subunit of human replication protein A and the role of the protein in DNA replication. J. Biol. Chem. **266:**12090–12098.
18. **Fairman, M. P., and B. Stillman.** 1988. Cellular factors required for multiple stages of SV40 DNA replication *in vitro*. EMBO J. **7:**1211–1218.
19. **Fotedar, R., and J. M. Roberts.** 1992. Cell cycle regulated phosphorylation of RPA-32 occurs within the replication initiation complex. EMBO J. **11:**2177–2187.
20. **Gottlieb, T. M., and S. P. Jackson.** 1993. The DNA-dependent protein kinase: requirement for DNA ends and association with Ku antigen. Cell **72:**131–142.
21. **He, Z., L. A. Henricksen, M. S. Wold, and J. C. Ingles.** 1995. RPA involvement in the damage-recognition and incision steps of nucleotide excision repair. Nature (London) **374:**566–569.
22. **Henricksen, L. A., C. B. Umbricht, and M. S. Wold.** 1994. Recombinant replication protein A: expression, complex formation, and functional characterization. J. Biol. Chem. **269:**11121–11132.
23. **Henricksen, L. A., and M. S. Wold.** 1994. Replication protein A mutants lacking phosphorylation sites for p34cdc2 kinase support DNA replication. J. Biol. Chem. **269:**24203–24208.
24. **Heyer, W.-D., M. R. S. Rao, L. F. Erdile, T. J. Kelly, and R. D. Kolodner.** 1990. An essential *Saccharomyces cerevisiae* single-stranded DNA binding protein is homologous to the large subunit of human RP-A. EMBO J. **9:** 2321–2329.
25. **Hosoda, J., and H. Moise.** 1978. Purification and physicochemical properties of limited proteolysis products of T4 helix destabilizing protein (gene 32 protein). J. Biol. Chem. **253:**7547–7558.
26. **Jackson, S. P., J. J. MacDonald, S. Lees-Miller, and R. Tjian.** 1990. GC box binding induces phosphorylation of Sp1 by a DNA-dependent protein kinase. Cell **63:**155–165.
27. **Kenny, M. K., S.-H. Lee, and J. Hurwitz.** 1989. Multiple functions of human single-stranded-DNA binding protein in simian virus 40 DNA replication: single-strand stabilization and stimulation of DNA polymerases α and δ. Proc. Natl. Acad. Sci. USA **86:**9757–9761.
28. **Kenny, M. K., U. Schlegel, H. Furneaux, and J. Hurwitz.** 1990. The role of human single-stranded DNA binding protein and its individual subunits in simian virus 40 DNA replication. J. Biol. Chem. **265:**7693–7700.
29. **Kim, C., B. F. Paulus, and M. S. Wold.** 1994. Interactions of human replication protein A with oligonucleotides. Biochemistry **33:**14197–14206.
30. **Kim, C., R. O. Snyder, and M. S. Wold.** 1992. Binding properties of replication protein A from human and yeast cells. Mol. Cell. Biol. **12:**3050–3059.
31. **Kirchgessner, C. U., C. K. Patil, J. W. Evans, C. A. Cuomo, L. M. Fried, T. Carter, M. A. Oettinger, and J. M. Brown.** 1995. DNA-dependent kinase (p350) as a candidate gene for the murine SCID defect. Science **267:**1178–1183.
32. **Lee, S.-H., and D.-K. Kim.** 1995. The role of the 34-kDa subunit of human replication protein A in simian virus 40 DNA replication in vitro. J. Biol. Chem. **270:**12801–12807.
33. **Lee, S.-H., D.-K. Kim, and R. Drissi.** 1995. Human xeroderma pigmentosum group A protein interacts with human replication protein A and inhibits DNA replication. J. Biol. Chem. **270:**21800–21805.
34. **Lee, S.-H., Z. Q. Pan, A. D. Kwong, P. M. J. Burgers, and J. Hurwitz.** 1991. Synthesis of DNA by DNA polymerase ε in vitro. J. Biol. Chem. **266:**22707–22717.
35. **Lees-Miller, S. P., Y.-R. Chen, and C. W. Anderson.** 1990. Human cells contain a DNA-activated protein kinase that phosphorylates simian virus 40 T antigen, mouse p53, and the human Ku autoantigen. Mol. Cell. Biol. **10:** 6472–6481.
36. **Lees-Miller, S. P., R. Godbout, D. W. Chan, M. Weinfeld, R. S. Day, G. M. Barron, and J. Allalunis-Turner.** 1995. Absence of p350 subunit of DNA-activated protein kinase from a radiosensitive human cell line. Science **267:** 1183–1185.
37. **Liu, V. F., and D. T. Weaver.** 1993. The ionizing radiation-induced replication protein A phosphorylation response differs between ataxia telangiectasia and normal human cells. Mol. Cell. Biol. **13:**7222–7231.
38. **Lohman, T. M., and M. E. Ferrari.** 1994. *Escherichia coli* single-stranded DNA-binding protein: multiple DNA binding modes and cooperativities. Annu. Rev. Biochem. **63:**527–570.
39. **Mastrangelo, I. A., A. J. Courey, J. S. Wall, S. P. Jackson, and P. V. C. Hough.** 1991. DNA looping and Sp1 multimer links: a mechanism for transcriptional synergism and enhancement. Proc. Natl. Acad. Sci. USA **88:**5670–5674.
40. **Mastrangelo, I. A., P. V. C. Hough, J. S. Wall, M. Dodson, F. B. Dean, and J. Hurwitz.** 1989. ATP-dependent assembly of double hexamers of SV40 T antigen at the viral origin of DNA replication. Nature (London) **338:**658–662.
41. **Matsuda, T., M. Saijo, I. Kuraoka, T. Kobayashi, Y. Nakatsu, A. Nagai, T. Enjoji, C. Masutani, K. Sugasawa, F. Hanaoka, A. Yasui, and K. Tanaka.**

1995. DNA repair protein XPA binds replication protein A (RPA). J. Biol. Chem. **270:**4152–4157.
42. **Melendy, T., and B. Stillman.** 1993. An interaction between replication protein A and SV40 T antigen appears essential for primosome assembly during SV40 DNA replication. J. Biol. Chem. **268:**3389–3395.
43. **Mitsis, P. G., S. C. Kowalczykowski, and I. R. Lehman.** 1993. A single-stranded DNA binding protein from *Drosophila melanogaster*: characterization of the heterotrimeric protein and its interaction with single-stranded DNA. Biochemistry **32:**5257–5266.
44. **Moore, S. P., L. Erdile, T. Kelly, and R. Fishel.** 1991. The human homologous pairing protein HPP-1 is specifically stimulated by the cognate single-stranded binding protein hRP-A. Proc. Natl. Acad. Sci. USA **88:**9067–9071.
45. **Morozov, V. E., M. Falzon, C. W. Anderson, and E. L. Kuff.** 1994. DNA-dependent protein kinase is activated by nicks and larger single-stranded gaps. J. Biol. Chem. **269:**16684–16688.
46. **Pan, Z.-Q., A. A. Amin, E. Gibbs, H. Niu, and J. Hurwitz.** 1994. Phosphorylation of the p34 subunit of human single-stranded-DNA-binding protein in cyclin A-activated G_1 extracts is catalyzed by cdk-cyclin A complex and DNA-dependent protein kinase. Proc. Natl. Acad. Sci. USA **91:**8343–8347.
47. **Pan, Z.-Q., C. H. Park, A. A. Amin, J. Hurwitz, and A. Sancar.** 1995. Phosphorylated and unphosphorylated forms of human single-stranded DNA-binding protein are equally active in simian virus 40 DNA replication and in nucleotide excision repair. Proc. Natl. Acad. Sci. USA **92:**4636–4640.
48. **Peterson, S. R., A. Kurimasa, M. Oshimura, W. S. Dynan, E. M. Bradbury, and D. J. Chen.** 1995. Loss of the catalytic subunit of the DNA-dependent protein kinase in DNA double-strand-break-repair mutant mammalian cells. Proc. Natl. Acad. Sci. USA **92:**3171–3174.
49. **Smider, V., W. K. Rathmell, M. R. Lieber, and G. Chu.** 1994. Restoration of x-ray resistance and V(D)J recombination in mutant cells by the Ku cDNA. Science **266:**288–291.
50. **Taccioli, G. E., T. M. Gottlieb, T. Blunt, A. Priestley, J. Demengeot, R. Mizuta, A. R. Lehmann, F. W. Alt, S. P. Jackson, and P. A. Jeggo.** 1994. Ku80: product of the XRCC5 gene and its role in DNA repair and V(D)J recombination. Science **265:**1442–1445.
51. **Tsurimoto, T., M. P. Fairman, and B. Stillman.** 1989. Simian virus 40 DNA replication in vitro: identification of multiple stages of initiation. Mol. Cell. Biol. **9:**3839–3849.
52. **Tsurimoto, T., and B. Stillman.** 1989. Multiple replication factors augment DNA synthesis by the two eukaryotic DNA polymerases, α and δ. EMBO J. **8:**3883–3889.
53. **Tucker, P. A., D. Tsernoglou, A. D. Tucker, F. E. Coenjaerts, H. Leenders, and P. C. van der Vliet.** 1994. Crystal structure of the adenovirus DNA binding protein reveals a hook-on model for cooperative DNA binding. EMBO J. **13:**2994–3002.
54. **Wall, J. S.** 1979. Biological scanning transmission electron microscopy, p. 333–342. *In* J. Hren, J. Goldstein, and D. Joy (ed.), Analytical electron microscopy. Plenum Press, New York.
55. **Williams, K. R., and W. Konigsberg.** 1978. Structural changes in the T4 gene 32 protein induced by DNA polynucleotides. J. Biol. Chem. **253:**2463–2470.
56. **Williams, K. R., E. K. Spicer, M. B. LoPresti, R. A. Guggenheimer, and J. W. Chase.** 1983. Limited proteolysis studies on the Escherichia coli single-stranded DNA binding protein. Evidence for a functionally homologous domain in both the Escherichia coli and T4 DNA binding proteins. J. Biol. Chem. **258:**3346–3355.
57. **Wobbe, C. R., L. Weissbach, J. A. Borowiec, F. B. Dean, Y. Murakami, P. Bullock, and J. Hurwitz.** 1987. Replication of simian virus 40 origin-containing DNA *in vitro* with purified proteins. Proc. Natl. Acad. Sci. USA **84:**1834–1838.
58. **Wold, M. S., and T. J. Kelly.** 1988. Purification and characterization of replication protein A, a cellular protein required for *in vitro* replication of simian virus 40 DNA. Proc. Natl. Acad. Sci. USA **85:**2523–2527.
59. **Wold, M. S., J. J. Li, and T. J. Kelly.** 1987. Initiation of simian virus 40 DNA replication *in vitro*: large-tumor-antigen- and origin-dependent unwinding of the template. Proc. Natl. Acad. Sci. USA **84:**3643–3647.
60. **Wold, M. S., D. H. Weinberg, D. M. Virshup, J. J. Li, and T. J. Kelly.** 1989. Identification of cellular proteins required for simian virus 40 DNA replication. J. Biol. Chem. **264:**2801–2809.